JACS
JOURNAL OF THE AMERICAN CHEMICAL SOCIETY

Article

pubs.acs.org/JACS

On the Energetics of Conformational Switching of Molecules at and Close to Room Temperature

Stefanie Ditze,[†,∥] Michael Stark,[†,∥] Florian Buchner,[†,∥,▽] André Aichert,[§] Norbert Jux,[⊥,∥] Nicola Luckas,[‡,∥] Andreas Görling,[‡,∥] Wolfgang Hieringer,[‡,∥] Joachim Hornegger,[§] Hans-Peter Steinrück,[†,∥] and Hubertus Marbach*[,†,∥]

[†]Lehrstuhl für Physikalische Chemie II and [‡]Lehrstuhl für Theoretische Chemie, Universität Erlangen-Nürnberg, Egerlandstr. 3, 91058 Erlangen, Germany

[⊥]Lehrstuhl für Organische Chemie II, Universität Erlangen-Nürnberg, Henkestr. 42, 91054 Erlangen, Germany

[∥]Interdisciplinary Center for Molecular Materials (ICMM) Universität Erlangen-Nürnberg, Germany

[§]Lehrstuhl für Mustererkennung, Universität Erlangen-Nürnberg, Martensstr. 3, 91058 Erlangen, Germany

[▽]Helmholtz Institut Ulm and Institut für Oberflächenchemie und Katalyse, Universität Ulm, Albert-Einstein Allee 47, 89069 Ulm, Germany

Supporting Information

ABSTRACT: We observe and induce conformational switching of individual molecules via scanning tunneling microscopy (STM) at and close to room temperature. 2H-5,10,15,20-Tetrakis-(3,5-di-*tert*-butyl)-phenylporphyrin adsorbed on Cu(111) forms a peculiar supramolecular ordered phase in which the molecules arrange in alternating rows, with two distinct appearances in STM which are assigned to concave and convex intramolecular conformations. Around room temperature, frequent bidirectional conformational switching of individual molecules from concave to convex and *vice versa* is observed. From the temperature dependence, detailed insights into the energy barriers and entropic contributions of the switching processes are deduced. At 200 K, controlled STM tip-induced unidirectional switching is possible, yielding an information storage density of 4.9×10^{13} bit/inch^2. With this contribution we demonstrate that controlled switching of individual molecules at comparably high temperatures is possible and that entropic effects can be a decisive factor in potential molecular devices at these temperatures.

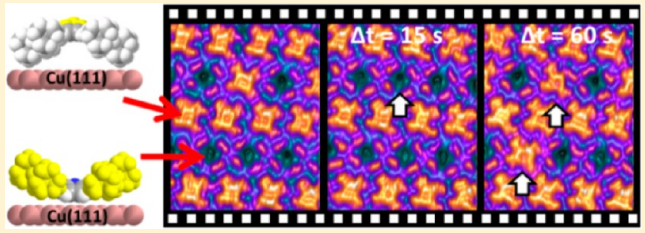

INTRODUCTION

An ultimate goal of nanotechnology is the usage of individual molecules or atoms as functional entities.[1,2] One important example is the application of switchable molecular building blocks in information storage.[3,4] In this context, the investigation of large organic molecules on well-defined surfaces in ultra-high vacuum has become a vivid research field with the vista to engineer functional devices. A large number of studies have been performed with scanning tunneling microscopy (STM) at low temperatures, which also opens up the possibility to directly investigate and/or manipulate molecular objects.[5−12] Various switching mechanisms have been investigated, like tautomerization of naphthalocyanine or 2H-porphyrin,[13,14] molecular cascades of CO molecules on Cu(111),[15] bond formation or cleavage in adsorbed molecules,[16−18] or generally conformational modifications[19−22] and specifically the well investigated trans−cis conformational change in azobenzene.[23−25] To prevent unwanted thermally induced processes, in particular the activation of these molecular switches or diffusion on the substrate, the corresponding experiments are usually conducted at temperatures well below 80 K, i.e., at temperatures outside the range for real applications. To engineer appropriate molecular switches, e.g., to design devices which can operate at higher temperatures, new molecular building blocks have to be evaluated, and a deeper understanding of the relevant mechanisms is required. One promising approach toward higher operation temperatures might be to target individual molecules within a self-assembled supramolecular array; in such an arrangement one can envisage to tailor the stability of a certain molecular conformation by the interplay between adsorbate−substrate and adsorbate−adsorbate interactions, and in addition diffusion can be effectively prevented.

EXPERIMENTAL SECTION

All experiments and sample preparation were performed in a two-chamber ultrahigh-vacuum system, at a background pressure in the low 10^{-10} mbar regime. The microscope is an RHK UHV VT STM 300 with RHK SPM 100 electronics. All given voltages refer to the sample, and the images have been taken in constant current mode. Moderate filtering (background subtraction and Gaussian smooth) of the STM

Received: November 21, 2013
Published: January 10, 2014

   dx.doi.org/10.1021/ja411884p | *J. Am. Chem. Soc.* 2014, 136, 1609−1616

data was performed for noise reduction. The Cu(111) single crystal was purchased from MaTeck. The preparation of the clean substrate surface was done by repeated cycles of Ar^+-ion sputtering (500 eV) and annealing to 850 K. 2H-5,10,15,20-Tetrakis-(3,5-di-*tert*-butyl)-phenylporphyrin (2HTTBPP) was prepared according to literature procedures starting from 3,5-bis-*tert*-butyl benzaldehyde and pyrrole.[26] The porphyrin layers were prepared by thermal sublimation at 620 K with a home-built Knudsen cell onto the substrate held at room temperature (RT). The STM data were processed with WSxM software.[27] A detailed description of the density calculations, of the temperature and drift control and the analysis of thermally induced switching as well as the determination of the internal conformation of 2HTTBPP can be found in the Supporting Information (SI).

RESULTS AND DISCUSSION

Herein, we demonstrate that in a well-defined self-assembled layer of 2HTTBPP on Cu(111), individual molecules can be switched from one specific conformation (convex) to another (concave) by the tip of an STM at 200 K. At higher temperatures, thermally induced switching occurs; from a statistical analysis of these switching events, the activation enthalpies and entropies are deduced, providing detailed insight into the switching process. We have chosen 2HTTBPP as molecular building block, since its macrocycle represents a planar framework as a structure forming element, and because the corresponding metalloporphyrins are well-known for their conformational flexibility and thus switching capabilities.[20,21,28−30] The Cu(111) surface appeared particularly suitable, since it was recently shown that it strongly interacts with the iminic nitrogen atoms of related free base porphyrins,[31,32] e.g., 2H-tetraphenylporphyrin (2HTPP).[33−36]

Figure 1a shows an overview STM image of a submonolayer of 2HTTBPP on Cu(111), with the molecules arranged in domains of alternating bright and dark rows. The high-resolution STM image in Figure 1b elucidates the dependence of the STM appearance of individual porphyrins on their intramolecular conformation. One can easily distinguish two types of appearances and assign them to the corresponding rows: the bright rows consist of molecules with a central protrusion and the dark rows of molecules with a central depression.

The periphery of the molecules appears as eight bright spots, which can be assigned to the eight *tert*-butyl substituents arranged in four groups around the molecular center corresponding to the four phenyl groups.[21,28,29]

As indicated in Figure 1b the four peripheral groups form a rectangle (indicated in green), which is basically identical for the two different molecular appearances. The geometry of the rectangle (aspect ratio of the short and long sides and perimeter) can be used to extract the intramolecular conformation with a method described elsewhere.[28] The corresponding conformation is described by twisting and/or tilting of the phenyl rings with respect to the porphyrin plane; the corresponding twist angle is denoted as θ and the tilt angle as ϕ (see SI for details). The estimated values of the two angles amount to $\theta = 5 \pm 5°$ and $\phi = 35 \pm 5°$ for both conformations, as sketched in Figure 1c,d. The visibility of all eight *tert*-butyl groups with similar apparent height also indicates that θ is indeed close to 0° and thus supports the estimated value of $5 \pm 5°$. Note that in a recent DFT study of the energy surface of the very similar CoTTBPP in the gas phase, a local minimum was located at very similar twist and tilt angles ($\theta = 10°$ and $\phi = 30°$), albeit at a relatively high energy.[30] In this conformation the molecule adopts a concave, bowl-like shape due to steric repulsions between the peripheral phenyl rings and the central pyrrole rings. Such conformations, which are rather exotic and energetically unfavorable in the gas phase, could be stabilized

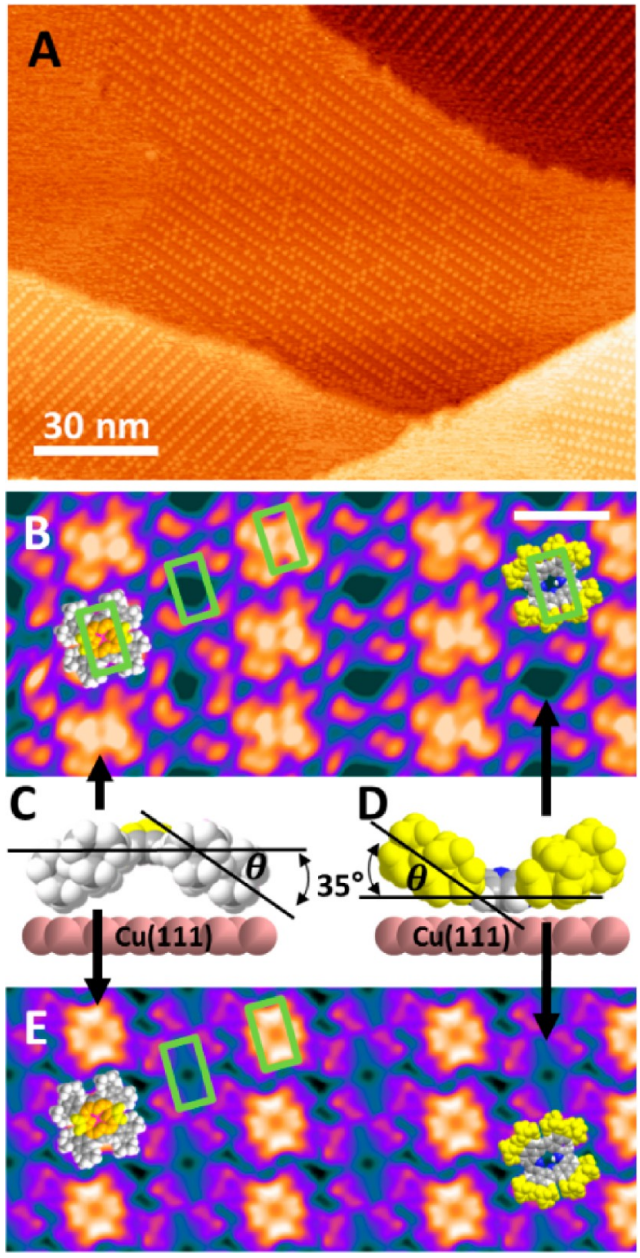

Figure 1. (a) STM image of ordered domains of 2HTTBPP on Cu(111) acquired at RT (U_{bias} = +1.31 V, I_{tunnel} = 30 pA). The molecules exhibit a bimodal appearance and are arranged in alternating rows. (b) High-resolution RT STM image (U_{bias} = +1.30 V, I_{tunnel} = 30 pA) of the supramolecular order shown in (a). The bright and dark rows in (a) consist of molecules with different intramolecular conformations, as indicated by the overlaid scaled models (top view). The scale bar represents 2 nm. (c, d) Space filling models of the convex (c) and concave (d) conformations of 2HTTBPP. The determination of the intramolecular conformation is based on the appearance in STM, in particular on the green rectangle formed by the peripheral substituents as indicated in the high-resolution ST micrographs. (e) Simulated STM image based on density functional electronic structure calculations of 2HTTBPP molecules in the conformations shown in (c) and (d) placed on a three layer Cu slab. Details of the simulation can be found in the SI.

dx.doi.org/10.1021/ja411884p | J. Am. Chem. Soc. 2014, 136, 1609−1616

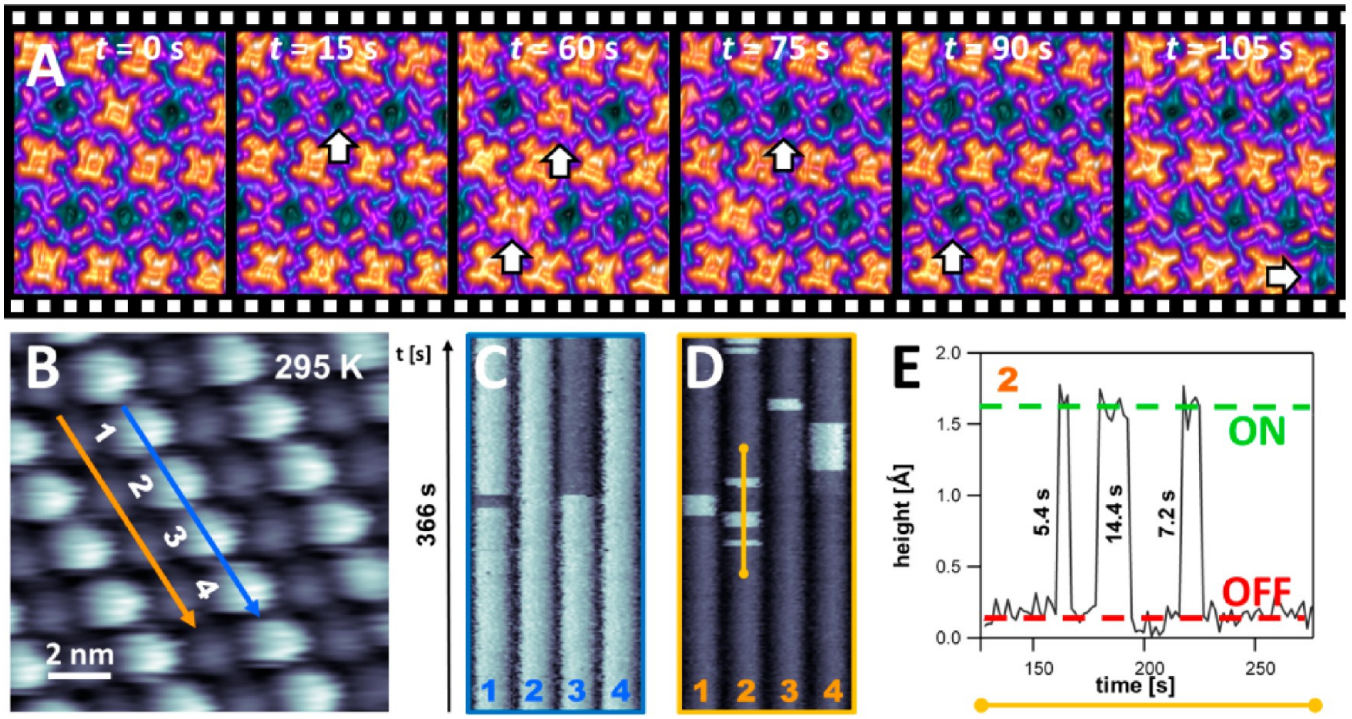

Figure 2. (a) Selected images from a high-resolution STM movie of a 2HTTBPP domain on Cu(111) acquired at RT (image to image acquisition time 15 s; U_{bias} = +1.76 V, I_{tunnel} = 24 pA). The arrows indicate individual molecules which exhibit a spontaneous conformational switching from concave to convex or *vice versa*. The times after acquisition of the first micrograph (left) are indicated by the *t* values. (b) Starting image of a "high-speed" STM movie (image to image acquisition time 1.8 s; U_{bias} = +1.30 V, I_{tunnel} = 30 pA) with reduced resolution but still robust contrast between concave and convex molecules. (c, d) Time evolution of two apparent height profiles of four molecules in the convex (c) and the concave row (d), extracted from "high speed" STM movie along the lines indicated in (b). Each contrast change at a given time (vertical direction) corresponds to one switching event. (e) Selected time evolution of the apparent height of molecule 2 in the concave row, extracted along the orange line in (d).

by molecule−substrate as well as lateral molecule−molecule interactions on a surface monolayer (see below).

Overall, our data suggest a bowl-like shape of the molecules with two distinctively different appearances in STM: in the dark row the molecules are in a concave conformation (bottom of the "bowl" on the surface, cf. Figure 1d), while in the bright row they are in a convex conformation (bowl is upside down, cf. Figure 1c). To crosscheck this interpretation we performed electronic structure calculations at the DFT level to simulate STM images of the molecules on a three-layer Cu slab; the molecular geometry has been chosen to resemble the experimentally determined conformation (for details see SI).

The simulated STM image depicted in Figure 1e mimics the main features of the experimental data very well and thus confirms the proposed intramolecular conformations. This type of pronounced bimodal appearance of a porphyrin derivative was not observed before; in particular, 2HTTBPP on Ag(111)[37] and CuTTBPP on Cu(111) (with θ = 75 ± 5° and ϕ = 0 ± 5°, i.e., similar to the overall minimum reported for CoTTBPP in the gas phase)[30] exhibits very different intra- and supramolecular conformations. A considerable attractive molecule−substrate interaction must account for the peculiar self-assembly of 2HTTBPP on Cu(111). The concave conformation is in line with the strong attractive interaction of the iminic nitrogen with Cu(111) for the smaller but closely related 2HTPP, such that the porphyrin macrocycle is "pulled" toward the surface.[33−36] Also, for molecules of this size attractive van der Waals interactions play a significant role (see the SI for dispersion-corrected DFT data).

In Figure 1a it becomes evident that the order within the rows is not perfect, i.e., in a row of concave molecules individual 2HTTBPPs exhibit the convex conformation and *vice versa*. Inspection of successive STM images of the same surface region at RT reveals that in both rows individual molecules occasionally change the conformation back and forth; a corresponding image series extracted from a high-resolution RT STM movie is shown in Figure 2a, with switching molecules indicated by the white arrows (see SI Movie M1). This behavior evidence the metastable nature of the intramolecular conformation at RT. In other words, a spontaneous reversible conformational switching of individual 2HTTBPP molecules occurs at RT.

This extraordinary behavior of 2HTTBPP on Cu(111) provides experimental access to the corresponding temperature-dependent switching dynamics and eventually gives a handle on the energetics of the switching by performing a suitable data analysis. For consecutively recorded images, the "image to image time" for the high-resolution imaging ($(12\ nm)^2$, 512^2 pixels), as depicted in Figure 2a, was 15 s.

To improve the time resolution, the scanning speed was increased, and the number of pixels was reduced to 128^2, leading to an "image to image time" of 1.8 s for $(12\ nm)^2$ images. The corresponding image in Figure 2b, recorded at 295 K, reveals that the concave and convex conformations of the individual molecules remain clearly distinguishable despite the lower resolution. The specific image was taken from a series of 200 consecutively recorded images with an overall time duration of 366 s. In the corresponding time lapse movie (see

dx.doi.org/10.1021/ja411884p | J. Am. Chem. Soc. 2014, 136, 1609−1616

SI Movie M3) one can observe occasional switching of molecules in both rows.

To visualize the switching events, time profiles were extracted from the STM movie, as indicated by the orange (concave row) and the blue (convex row) lines in Figure 2b, such that four molecules per row can be traced. In Figure 2c,d the considered molecules in the concave and convex row, respectively, are labeled with numbers (1−4,) and the profiles are plotted against time, from bottom to top, in a standard gray scale (bright: high apparent height, dark: reduced apparent height).

Each abrupt change in contrast along the vertical direction (time) corresponds to one switching event. A close-up on the time-dependent conformational switching of molecule 2 in the concave row is given in Figure 2e. Here the apparent height in STM is plotted against time. One can immediately distinguish two height levels differing by ∼1.5 Å and correlate them to the corresponding molecular conformers.

Thus, each molecule constitutes a two-state system, in which the two states can be assigned to arbitrary values like "on" and "off", as indicated in Figure 2e, or correspondingly "1" and "0" for binary information storage, which is of great interest in the context of future devices for information storage. Altogether six switching events are shown, which result in three periods where the molecule is not in the native conformation of its row (here concave). The corresponding lifetimes of the convex state (indicated in Figure 2e) range from 5.4 to 14.4 s and are thus well above the time resolution of 1.8 s of the STM movie.

In order to address the temperature dependence of the switching behavior, such STM time series were recorded at different temperatures. Figure 3 shows representative data sets of four molecules in a convex (top) and in a concave (bottom) row for 270, 295, and 320 K. In both rows the number of switching events increases with temperature, and at the same time the lifetime of the deviant state within the rows decreases. Interestingly, the switching frequency in the concave row is much higher than in the convex row.

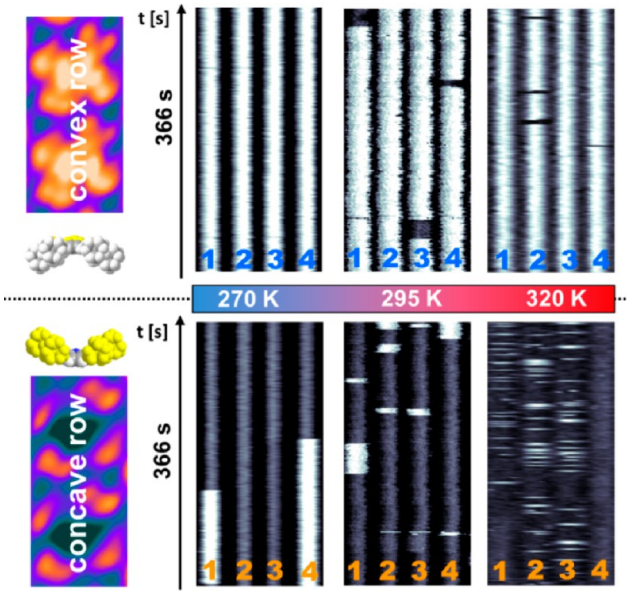

Figure 3. Visualization of thermally induced conformational switching in a convex (upper part) and a concave row (bottom part) at 270, 295, and 320 K (cf. Figure 2b−e). The data are extracted from corresponding time lapse STM movies (U_{bias} = +1.30 V, I_{tunnel} = 30 pA). The representative samples illustrate that the molecules in the concave row switch more frequently, which is particularly evident at 320 K.

This is unexpected at first sight, since the strong attractive interaction of the iminic nitrogen of the 2HTTBPP with the substrate as well as significant van der Waals forces (see the SI) suggest a higher energy barrier to switch the molecules in the concave row than in the convex row.

To gain further insight into the thermally driven switching process we performed a quantitative analysis of corresponding isothermal STM movies acquired at five temperatures between 280 and 300 K. The upper limit of 300 K was chosen such that the observed switching processes are still slower than the time resolution of ∼1.8 s of the STM movie data, i.e., such that no switching events are missed. At temperatures lower than 280 K the number of switching events was too low to collect conclusive data. The corresponding STM image sequences allow for the identification of switching events from the "native" state to the "deviant" state and back, in both the concave and the convex rows.

In other words, we distinguish four different switching events and analyze them separately (cf. Figure 4). To do so, STM movies were analyzed using a semiautomatic image processing tool developed for this purpose (see SI). This tool enabled the determination of more than 1.5 million molecular conformations from more than altogether 70 000 STM images, acquired in the temperature range of 280−300 K. From this database we extracted more than 10 000 switching events. The switching rates r were determined as the number of switching events divided by the lifetimes of the corresponding four states (see SI for details).

The observed increase of the switching rate with temperature indicates that the intramolecular conformation change is an activated process. Typically, such activated processes are analyzed using an Arrhenius plot, yielding the activation energy E and the corresponding prefactor A. The drawback of this analysis is that it does not provide physical insight into the nature of the prefactor, which is particularly desired when major changes in the entropy of the different states occur.

An alternative approach described in detail by Winzor et al.[38] refers to the original formulation of transition-state theory (TST) in which the Gibbs energy defines the activation barrier to be overcome.[39] The rate r for an activated process is then given by

$$r = \kappa\left(\frac{k_B T}{h}\right)\cdot e^{-\Delta G^{\ddagger}/k_B T}$$

with κ being the transmission factor, which is usually set to κ = 1.[38] With the Gibbs−Helmholtz equation the enthalpic ($\Delta H^{\ddagger}$) and entropic ($T\Delta S^{\ddagger}$) contributions of the Gibbs energy are given as $\Delta G^{\ddagger} = \Delta H^{\ddagger} - T\Delta S^{\ddagger}$ and the rate constant can be expressed as the so-called Eyring equation:

$$r = \kappa\left(\frac{k_B T}{h}\right)\cdot e^{\Delta S^{\ddagger}/k_B} e^{-\Delta H^{\ddagger}/k_B T}$$

The logarithmic form of the Eyring equation divided by T is

$$\ln\left(\frac{r}{T}\right) = \ln(\kappa) + \ln\left(\frac{k_B}{h}\right) + \frac{\Delta S^{\ddagger}}{k_B} - \frac{\Delta H^{\ddagger}}{k_B T}$$

dx.doi.org/10.1021/ja411884p | J. Am. Chem. Soc. 2014, 136, 1609−1616

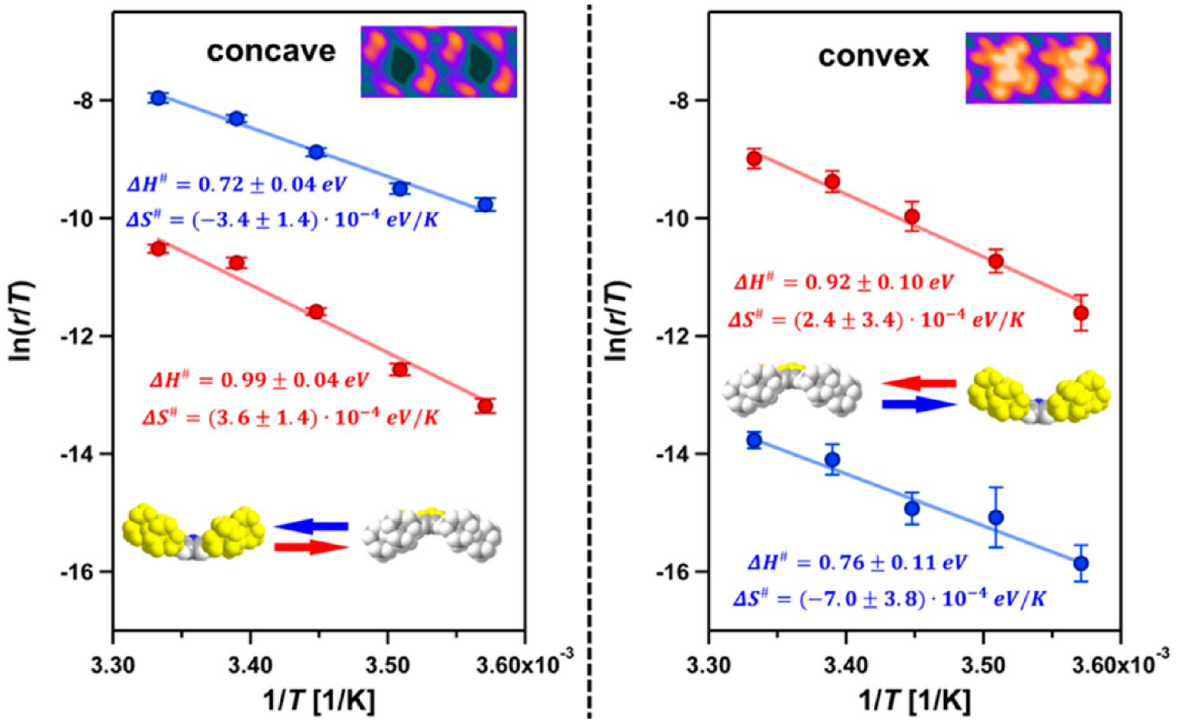

Figure 4. Plots of $\ln(r/T)$ vs $1/T$ for the two switching events (concave to convex in red and convex to concave in blue) in the concave row (left-hand side) and in the convex row (right-hand side). The corresponding $\Delta H^{\ddagger}$ and $\Delta S^{\ddagger}$ values determined from linear regressions are given in the same color code. The error bars represent the standard error.

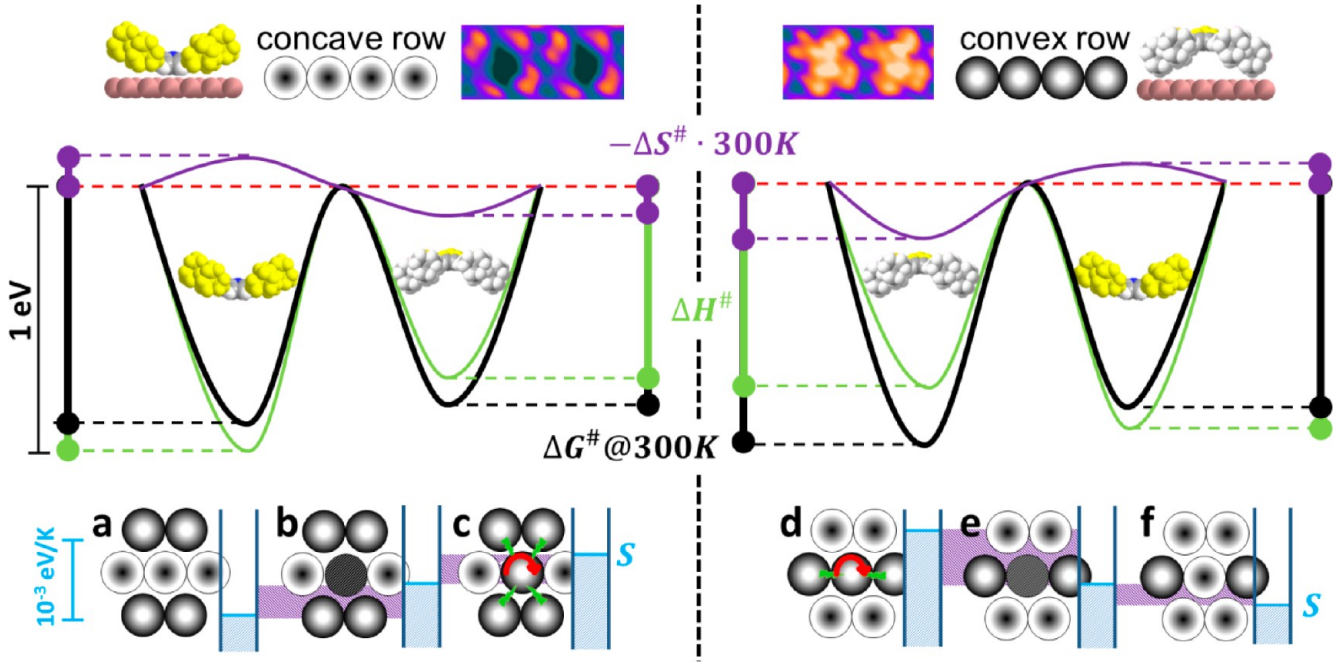

Figure 5. Sketch of the thermodynamic potential differences at 300 K (vertical bars) and the resulting energy landscape for conformational switching of 2HTTBPP on Cu(111) in the concave (left side) and the convex row (right side). The curve which determines the switching behavior is the one for $\Delta G^{\ddagger}$ drawn in black. The free energy difference is composed of contributions from $\Delta H^{\ddagger}$ and $-\Delta S^{\ddagger}\cdot 300$ K, displayed in green and purple, respectively. Please note that by reducing the temperature the free energy value will shift toward the enthalpy value, i.e., at 0 K the black curve coincides with the green one. In the bottom row schematics of the central molecule in the convex (c, d: central bright spot), the transition state (b, e: black) and the concave conformation (a, f: central dark spot), along with their next neighbors, are depicted. The height of the blue bar indicates the entropy values S, and the purple bars mark the corresponding entropy differences $\Delta S^{\ddagger}$ as extracted from the data depicted in Figure 4 and directly related to the $-\Delta S^{\ddagger}\cdot 300$ K values above (also printed in purple). The observed entropy increase from concave over the transition state to convex can be explained by the strong molecule−substrate interaction in the concave conformation going along with reduced degrees of freedom. Exemplary, the rotation of convex molecules is indicated by the red arrows in the scheme (c, d); the green flashes (c, d) indicate steric hindrance by next neighbor molecules with the same convex conformation and thus reduced rotation, i.e., smaller entropy.

dx.doi.org/10.1021/ja411884p | J. Am. Chem. Soc. 2014, 136, 1609−1616

By plotting $\ln(r/T)$ as a function of $1/T$ one can extract the slope $m = -\Delta H^{\ddagger}/k_B$ and the ordinate intercept $y = \ln(k_B/h) + (\Delta S^{\ddagger}/k_B)$, with κ set to unity and thus $\ln(\kappa) = 0$.

In Figure 4, the corresponding data are shown for the switching events in the concave rows (left) and the convex rows (right), as derived from the isothermal STM measurements. For both rows, the data for switching from the concave to the convex conformation and *vice versa* are shown. The lines represent the corresponding least-squares fits; furthermore, the resulting values for $\Delta H^{\ddagger}$ and $\Delta S^{\ddagger}$ are given.

The comparison of the enthalpic barriers for both rows shows that the barriers to overcome for the transition from concave to convex are the same within the margin of errors ($\Delta H^{\ddagger} = 0.92 \pm 0.10$ vs 0.99 ± 0.04 eV; in red). The same holds for the reverse switching direction, i.e., from convex to concave (0.76 ± 0.11 vs 0.72 ± 0.04 eV; in blue). In other words, the enthalpic barrier, $\Delta H^{\ddagger}$, is the same for the same transition in the two different rows. Remarkably, the enthalpic barrier for switching from concave to convex (red) is ~30% higher than for the opposite direction (blue). This is in line with the strong attractive interaction of the concave molecule with the substrate, as discussed above (see also the SI). Despite the stronger interaction, the switching frequency is larger in the concave row, which must be due to entropic contributions.

In Figure 5, the Gibbs energy scheme, with the derived thermodynamic potentials, $\Delta H^{\ddagger}$ (green), $T\Delta S^{\ddagger}$ (purple), and the resulting $\Delta G^{\ddagger}$ (black), is sketched for a temperature of 300 K. Following the Gibbs–Helmholtz equation, $\Delta S^{\ddagger}$ contributes as $-T\Delta S^{\ddagger}$ to $\Delta G^{\ddagger}$, i.e., positive entropy differences lower the Gibbs energy barrier as plotted in Figure 5. Considering just $\Delta H^{\ddagger}$ (green), in the convex row the concave conformation would be clearly favored, as expected from the stronger binding to the surface. However, with the entropic contribution $-T\Delta S^{\ddagger}$ (violet) to the Gibbs energy the convex state becomes favorable (black). In other words, convex molecules in the convex rows and thus the whole supramolecular arrangement are entropically stabilized at 300 K. In the concave row, the entropic contributions also lead to some destabilization of the enthalpically favored concave conformation (green) but do not reverse the stability in terms of the Gibbs energy (black).

To further investigate the entropic effects, we discuss STM results acquired at 200 K, where thermally induced switching does not occur. However, the situation is not a static one, but in STM movies we observe that convex 2HTTBPP molecules (irrespective of their molecular neighborhood) frequently change their appearance and azimuthal orientation, indicating that they rotate around the surface normal already at 200 K and that vibrational degrees of freedom and also frustrated translations are excited (see SI, Figure S3 and movie M5). At the same time, the concave molecules appear rather static, which can be understood considering the stronger molecule–substrate interaction via the iminic nitrogen atoms (as discussed above), which also hinders rotational motion. This may furthermore lead to an enhanced lateral confinement and possibly also to energetically less accessible vibrational motions due to a stiffening of the whole molecule. As a consequence, the rotational, vibrational, and frustrated translational entropy values of the convex molecules are larger than those of the concave ones. The influence of rotational entropy on the behavior of larger organic molecules was recently investigated in detail in temperature programmed desorption experiments partially combined with STM.[40−43] For example, Waldmann et al. found large differences in the prefactor for desorption, depending on the rotational state before desorption:[41] For a molecule, which rotates in the adsorbed state on the surface, a smaller entropy difference to a desorbed molecule in the gas phase was found than for the same molecule, which is not rotating in the adsorbed state. Following the route described by Waldmann et al., we estimate the rotational entropy for a 2HTTBPP molecule freely rotating around an axis perpendicular to the surface plane.[41] The moment of inertia of the 2HTTBPP around the axis through the center of the molecule is estimated to $I_z = 8.79 \times 10^{-43}$ kg·m^2. From this value the partition function at 300 K is determined from

$$z_{\mathrm{rot}}^{\mathrm{ads}} = \frac{1}{\sigma\sqrt{\pi}}\left(\frac{8\pi^2 k_B T}{h^2}\right)^{1/2}(I_z)^{1/2}$$

to be $z_{\mathrm{rot}}^{\mathrm{ads}}$. The corresponding rotational entropy value is then calculated to 5.1×10^{-4} eV K^{-1} using

$$S_{\mathrm{rot}}^{\mathrm{ads}} = k_B\left[\frac{1}{2} + \ln(z_{\mathrm{rot}}^{\mathrm{ads}})\right]$$

This number corresponds to an equivalent energy value of 0.153 eV at 300 K, representing the difference between a freely rotating and a nonrotating 2HTTBPP. This value is certainly only an upper estimate for the actual value since the convex molecule is not expected to rotate freely in the supramolecular structure.

In our analysis, the entropy difference between the convex and concave conformation of 2HTTBPP in the convex row is 9.4×10^{-4} eV·K^{-1}, which corresponds to an energy value of 0.28 eV at 300 K. The calculated rotational entropy value of 0.15 eV is ~55% of the latter value. Considering that, along with the rotation, other degrees of freedom like vibrations and frustrated translations contribute to entropy difference between the convex and concave conformations, we exemplarily focus on the rotation to qualitatively explain the entropy differences. The bottom part of Figure 5 schematically illustrates the explanation for the entropy differences by sketching the respective molecule with all six next neighbors in the supramolecular environment. Our conjecture is that the concave molecules (Figure 5a,f) generally have much smaller entropy than the convex ones (Figure 5c,d), as explained above. The convex molecules are able to rotate in the supramolecular structure (indicated by red arrows in Figure 5c,d). Thereby neighboring molecules act as a "bearing" for the rotational motion.[44] We infer from the data and simple steric considerations that neighboring molecules in the same conformation hinder rotation, and also other motions, due to steric repulsions. Hence, with increasing number of next neighbors with the same convex conformation (indicated with green flashes in Figure 5c,d) the degree of freedom of motion and thus the entropy will decrease. In this way, the rotational motion observed for the convex molecules is increasingly frustrated with increasing number of neighbors in convex conformation. In other words, the rotational entropy of a convex molecule with four convex neighbors in the neighboring rows (Figure 5c) is lower than that of a convex molecule which has only two convex neighbors (Figure 5d). From these considerations, i.e., by accounting for conformation and molecular neighborhood, the magnitudes of the corresponding entropies directly result as indicated by the blue bars.

Finally, we demonstrate that individual porphyrin molecules can be switched with the STM tip. The corresponding

experiments were performed at 200 K to effectively prevent thermally induced switching. In Figure 6, a sequence of STM images is displayed, illustrating that we can indeed switch individual molecules in the convex rows from the convex to the concave conformation (i.e., from bright to dark) using comparably high bias voltages and local electron doses: To induce the conformational change, the tip was positioned above a particular convex molecule (left molecule in top row in Figure 6). Upon increasing the bias voltage U_{bias} from +1.30 to +1.75 V for 5 s (keeping the feedback loop closed and maintaining I_{tunnel} = 30 pA), the molecule is switched to the concave conformation (second row). Thereafter, the tip was positioned above the next molecule (central molecule in second row), which was again switched by applying a voltage pulse. Note that for lower U_{bias} values between +1.4 and +1.6 V for 5−30 s no switching from convex to concave was observed.

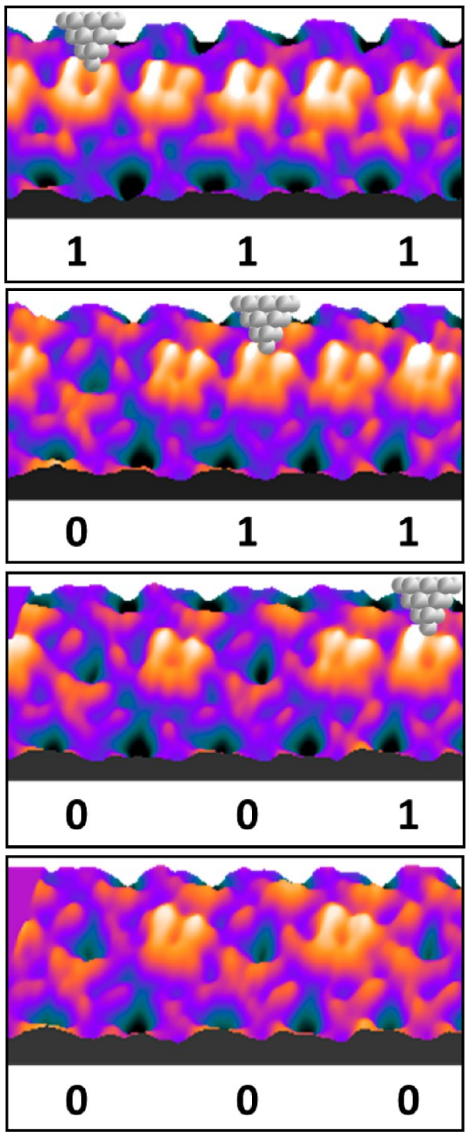

Figure 6. STM tip-induced conformational switching of individual molecules in the convex rows. The STM images are all acquired with U_{bias} = +1.30 V and I_{tunnel} = 30 pA. For switching the tip was placed over a convex molecule for 5 s with U_{bias} = +1.75 V. The tip positions before applying the voltage pulse are indicated in the images as schematic STM tip. In the subsequent images (from top to bottom) the molecules exhibit the concave conformations. Switching is restricted to the convex molecules. While the supramolecular structure breaks down upon switching of neighboring molecules, it remains intact switching every second molecules, as shown here. In this way binary information can be stored as indicated as "0" and "1" at the bottom of the images, yielding an information storage density of 4.9×10^{13} bit/inch^2.

By studying the switching process systematically, we found that consecutive switching of directly neighboring molecules in a convex row leads to the destruction of the local supramolecular order. However, switching every second molecule in the convex row, as done in Figure 6, leaves the supramolecular arrangement intact and thus is suitable for information storage with a very high information storage density of 4.9×10^{13} bit/inch^2.

Interestingly, we never succeeded to switch in the other direction, i.e., from concave to convex. This can partly be understood considering that the entropic contributions to the activation barrier decrease with temperature, and thus the energy landscape of the free energy (black in Figure 5) will shift toward the enthalpy contribution (green in Figure 5) until both curves merge at 0 K. In other words, both the entropic stabilization of the convex conformation and the entropic destabilization of the concave conformation diminish with decreasing temperature, and thus the concave conformation becomes increasingly favorable also in the convex row. As a consequence the free energy barrier for switching from convex to concave is reduced, and thus the corresponding tip-induced switching is facilitated. Apart from this thermodynamic consideration, it is clear that the tip-induced switching is based on the impact of the tunneling electron, and therefore also other processes like cross sections for inelastic electron excitations or relaxation channels for exited states in the molecule will play an important role. We propose that the discussed strong coupling of the concave molecules with the substrate provides an effective decay channel for tip-induced excitations, which leads to a quenching of the switching from concave to convex conformation.

CONCLUSIONS

In summary, we provide detailed insight into the process of thermally induced switching. At higher temperatures, entropic stabilization effects can dominate the stability of specific molecular conformations on the surface and also the resulting switching behavior. Furthermore, our results demonstrate that the conformational switching of individual molecules using voltage pulses from an STM at 200 K is possible, yielding a very high information storage density of 4.9×10^{13} bit/inch^2. This considerably expands the field of STM tip-induced switching to higher temperatures, which is a crucial and important step toward the development of molecular switching devices for RT applications. As an outlook, we propose to further explore this type of supramolecular systems with tailor-made porphyrin derivatives not only to enable controlled tip-induced molecular switching at RT but also to further investigate fundamental questions concerning the role of the thermodynamic potentials in such processes.

ASSOCIATED CONTENT

Supporting Information

Additional figures and results including temperature and drift control, the analysis of thermally induced switching, the determination of the internal conformation of 2HTTBPP, and density functional calculations as well as a description of

dx.doi.org/10.1021/ja411884p | J. Am. Chem. Soc. 2014, 136, 1609−1616

the evaluation software. Further STM time-lapse movies are available. This material is available free of charge via the Internet at http://pubs.acs.org.

AUTHOR INFORMATION

Corresponding Author

hubertus.marbach@fau.de

Notes

The authors declare no competing financial interest.

ACKNOWLEDGMENTS

The authors thank the German Science Foundation (DFG) for financial support through SFB 583 and the Excellence Cluster "Engineering of Advanced Materials" granted to the Friedrich-Alexander Universität Erlangen-Nürnberg.

REFERENCES

(1) Barth, J. V.; Costantini, G.; Kern, K. *Nature* **2005**, *437*, 671.
(2) Joachim, C.; Gimzewski, J. K.; Aviram, A. *Nature* **2000**, *408*, 541.
(3) Carroll, R. L.; Gorman, C. B. *Angew. Chem., Int. Ed.* **2002**, *41*, 4378.
(4) Green, J. E.; Wook Choi, J.; Boukai, A.; Bunimovich, Y.; Johnston-Halperin, E.; DeIonno, E.; Luo, Y.; Sheriff, B. A.; Xu, K.; Shik Shin, Y.; Tseng, H.-R.; Stoddart, J. F.; Heath, J. R. *Nature* **2007**, *445*, 414.
(5) Foster, J. S.; Frommer, J. E.; Arnett, P. C. *Nature* **1988**, *331*, 324.
(6) Grill, L. *J. Phys.: Condens. Matter* **2008**, *20*, 053001.
(7) Ho, W. *J. Chem. Phys.* **2002**, *117*, 11033.
(8) Nazin, G. V.; Qiu, X. H.; Ho, W. *Science* **2003**, *302*, 77.
(9) Qiu, X. H.; Nazin, G. V.; Ho, W. *Science* **2003**, *299*, 542.
(10) Schaffert, J.; Cottin, M. C.; Sonntag, A.; Karacuban, H.; Bobisch, C. A.; Lorente, N.; Gauyacq, J.-P.; Moeller, R. *Nat. Mater.* **2013**, *12*, 223.
(11) Wang, Y. F.; Kröger, J.; Berndt, R.; Hofer, W. A. *J. Am. Chem. Soc.* **2009**, *131*, 3639.
(12) Morgenstern, K. *Surf. Interface Anal.* **2010**, *42*, 1634.
(13) Auwärter, W.; Seufert, K.; Bischoff, F.; Ecija, D.; Vijayaraghavan, S.; Joshi, S.; Klappenberger, F.; Samudrala, N.; Barth, J. V. *Nat. Nanotechnol.* **2012**, *7*, 41.
(14) Liljeroth, P.; Repp, J.; Meyer, G. *Science* **2007**, *317*, 1203.
(15) Heinrich, A. J.; Lutz, C. P.; Gupta, J. A.; Eigler, D. M. *Science* **2002**, *298*, 1381.
(16) Maksymovych, P.; Sorescu, D. C.; Jordan, K. D.; Yates, J. T. *Science* **2008**, *322*, 1664.
(17) Mohn, F.; Repp, J.; Gross, L.; Meyer, G.; Dyer, M. S.; Persson, M. *Phys. Rev. Lett.* **2010**, *105*, 266102.
(18) Piantek, M.; Schulze, G.; Koch, M.; Franke, K. J.; Leyssner, F.; Krueger, A.; Navio, C.; Miguel, J.; Bernien, M.; Wolf, M.; Kuch, W.; Tegeder, P.; Pascual, J. I. *J. Am. Chem. Soc.* **2009**, *131*, 12729.
(19) Iancu, V.; Hla, S.-W. *Proc. Natl. Acad. Sci. U.S.A.* **2006**, *103*, 13718.
(20) Loppacher, C.; Guggisberg, M.; Pfeiffer, O.; Meyer, E.; Bammerlin, M.; Luthi, R.; Schlittler, R.; Gimzewski, J. K.; Tang, H.; Joachim, C. *Phys. Rev. Lett.* **2003**, *90*, 066107.
(21) Moresco, F.; Meyer, G.; Rieder, K. H.; Tang, H.; Gourdon, A.; Joachim, C. *Phys. Rev. Lett.* **2001**, *86*, 672.
(22) Yanagi, H.; Ikuta, K.; Mukai, H.; Shibutani, T. *Nano Lett.* **2002**, *2*, 951.
(23) Alemani, M.; Peters, M. V.; Hecht, S.; Rieder, K.-H.; Moresco, F.; Grill, L. *J. Am. Chem. Soc.* **2006**, *128*, 14446.
(24) Safiei, A.; Henzl, J.; Morgenstern, K. *Phys. Rev. Lett.* **2010**, *104*, 216102.
(25) Wolf, M.; Tegeder, P. *Surf. Sci.* **2009**, *603*, 1506.
(26) Miyamoto, T. K.; Sugita, N.; Matsumoto, Y.; Sasaki, Y.; Konno, M. *Chem. Lett.* **1983**, *12*, 1695.
(27) Horcas, I.; Fernandez, R.; Gomez-Rodriguez, J. M.; Colchero, J.; Gomez-Herrero, J.; Baro, A. M. *Rev. Sci. Instrum.* **2007**, *78*, 013705.
(28) Buchner, F.; Comanici, K.; Jux, N.; Steinrück, H.-P.; Marbach, H. *J. Phys. Chem. C* **2007**, *111*, 13531.
(29) Jung, T. A.; Schlittler, R. R.; Gimzewski, J. K. *Nature* **1997**, *386*, 696.
(30) Wölfle, T.; Görling, A.; Hieringer, W. *Phys. Chem. Chem. Phys.* **2008**, *10*, 5739.
(31) González-Moreno, R.; Sánchez-Sánchez, C.; Trelka, M.; Otero, R.; Cossaro, A.; Verdini, A.; Floreano, L.; Ruiz-Bermejo, M.; García-Lekue, A.; Martín-Gago, J. Á.; Rogero, C. *J. Phys. Chem. C* **2011**, *115*, 6849.
(32) Haq, S.; Hanke, F.; Dyer, M. S.; Persson, M.; Iavicoli, P.; Amabilino, D. B.; Raval, R. *J. Am. Chem. Soc.* **2011**, *133*, 12031.
(33) Buchner, F.; Xiao, J.; Zillner, E.; Chen, M.; Röckert, M.; Ditze, S.; Stark, M.; Steinrück, H.-P.; Gottfried, J. M.; Marbach, H. *J. Phys. Chem. C* **2011**, *115*, 24172.
(34) Diller, K.; Klappenberger, F.; Marschall, M.; Hermann, K.; Nefedov, A.; Woll, C.; Barth, J. V. *J. Chem. Phys.* **2012**, *136*, 014705.
(35) Ditze, S.; Stark, M.; Drost, M.; Buchner, F.; Steinrück, H.-P.; Marbach, H. *Angew. Chem., Int. Ed.* **2012**, *51*, 10898.
(36) Rojas, G.; Chen, X.; Bravo, C.; Kim, J.-H.; Kim, J.-S.; Xiao, J.; Dowben, P. A.; Gao, Y.; Zeng, X. C.; Choe, W.; Enders, A. *J. Phys. Chem. C* **2010**, *114*, 9408.
(37) Buchner, F. *STM Investigation of Molecular Architectures of Porphyrinoids on a Ag(111) Surface: Supramolecular Ordering, Electronic Properties and Reactivity*; 1 ed.; Springer-Verlag: Heidelberg, 2010.
(38) Winzor, D. J.; Jackson, C. M. *J. Mol. Recognit.* **2006**, *19*, 389.
(39) Laidler, K. J.; Glasstone, S.; Eyring, H. *J. Chem. Phys.* **1940**, *8*, 659.
(40) Roos, M.; Breitruck, A.; Hoster, H. E.; Behm, R. J. *Phys. Chem. Chem. Phys.* **2010**, *12*, 818.
(41) Waldmann, T.; Klein, J.; Hoster, H. E.; Behm, R. J. *ChemPhysChem* **2013**, *14*, 162.
(42) Campbell, C. T.; Sellers, J. R. V. *J. Am. Chem. Soc.* **2012**, *134*, 18109.
(43) Paserba, K. R.; Gellman, A. J. *Phys. Rev. Lett.* **2001**, *86*, 4338.
(44) Gimzewski, J. K.; Joachim, C.; Schlittler, R. R.; Langlais, V.; Tang, H.; Johannsen, I. *Science* **1998**, *281*, 531.